BEAMLET PULSE-GENERATION AND WAVEFRONT-CONTROL SYSTEM

B. M. Van Wonterghem

J. T. Salmon

R. W. Wilcox

Introduction

The Beamlet pulse-generation system (or "front end") refers to the laser hardware that generates the spatially and temporally shaped pulse that is injected into the main laser cavity. All large ICF lasers have pulse-generation systems that typically consist of a narrow-band oscillator, electro-optic modulators for temporal and bandwidth shaping, and one or more preamplifiers. Temporal shaping is used to provide the desired laser output pulse shape and also to compensate for gain saturation effects in the large-aperture amplifiers. Bandwidth is applied to fulfill specific target irradiation requirements and to avoid stimulated Brillouin scattering (SBS) in large-aperture laser components. Usually the sharp edge of the beam's spatial intensity profile is apodized before injection in the main amplifier beam line. This prevents large-amplitude ripples on the intensity profile.

Beamlet's pulse-generation system provides the same functions as stated, but uses entirely new technology. For example, compact diode-pumped oscillators and integrated optical-waveguide modulators, in combination with a high-gain multipass preamplifier, replace typical room-sized systems, such as used on Nova[1,2] and other ICF lasers. In addition, the Beamlet front end provides a new feature of extensive precompensation for gain nonuniformity in the cavity and booster amplifiers. It also corrects for static and dynamic (pump-induced) phase aberrations in the entire laser chain.

The newly developed Beamlet front end significantly increases the quality of the output beam of a large-amplifier chain and is essential to the National Ignition Facility's (NIF's) conceptual design. (See "System Description and Initial Performance Results for Beamlet," p. 1.) Compensation for optical phase aberrations increases the frequency conversion efficiency and the brightness, and hence the 3ω peak power at the focus of the target chamber. Correction for spatial amplifier gain variations improves the output beam intensity uniformity and thereby increases the aperture fill-factor and the total output energy per beam line. The compact integrated optics approach to temporal shaping allows precise control over individual pulse shapes, which improves control of power balance and irradiation uniformity in a multiple-beam target irradiation scheme such as NIF.

Beamlet's pulse-generation system has proven to be very flexible and reliable in operation with minimal operator intervention; Table 1 summarizes the current performance limits and nominal operating points for this system.

Many aspects of the Beamlet front end are described in other publications.[1,2] In this article, we briefly review the front-end design and discuss improvements to the oscillator and modulator systems. Our main focus, however, is to describe Beamlet's novel beam-shaping and wavefront-control systems that have recently been fully activated and tested.

TABLE 1. Beamlet's front-end performance limits and nominal operating points.

	Maximum	Typical
Energy (3 ns pulse duration)	12 J	1 J
Pulse duration	0.2–10* ns	3 ns
Temporal shaping contrast	100:1	5:1
Bandwidth	100 GHz	32 GHz
Center-to-edge intensity profile ratio	0.2	0.3
Wavefront shaping	±4λ	>3λ peak to valley

*Limited by length of regenerative amplifier cavity.

UCRL-LR-105821-95-1

Beamlet Front-End Description

Figure 1 shows the detailed layout of the Beamlet front-end oscillator and preamplifier. A single-mode oscillator generates high-rep-rate pulses, which are coupled into a single-mode polarization preserving fiber. The fiber couples the light into an integrated high-speed amplitude and phase modulator. Control signals are generated by low-voltage electronic pulse generators. The resulting shaped pulse is transported to the preamplifier section in the laser high-bay using a 60-m-long fiber. A ring regenerative amplifier provides a gain of 10^9 to elevate the energy to the millijoule level. At this point, the Gaussian spatial intensity is flattened and shaped into a one-dimensional (1-D) parabolic intensity profile. A square serrated aperture creates the desired spatial edge shape for injection in the main amplifier. A second four-pass rod amplifier boosts the energy to the joule-level and two 10-cm-aperture Faraday rotators provide isolation against

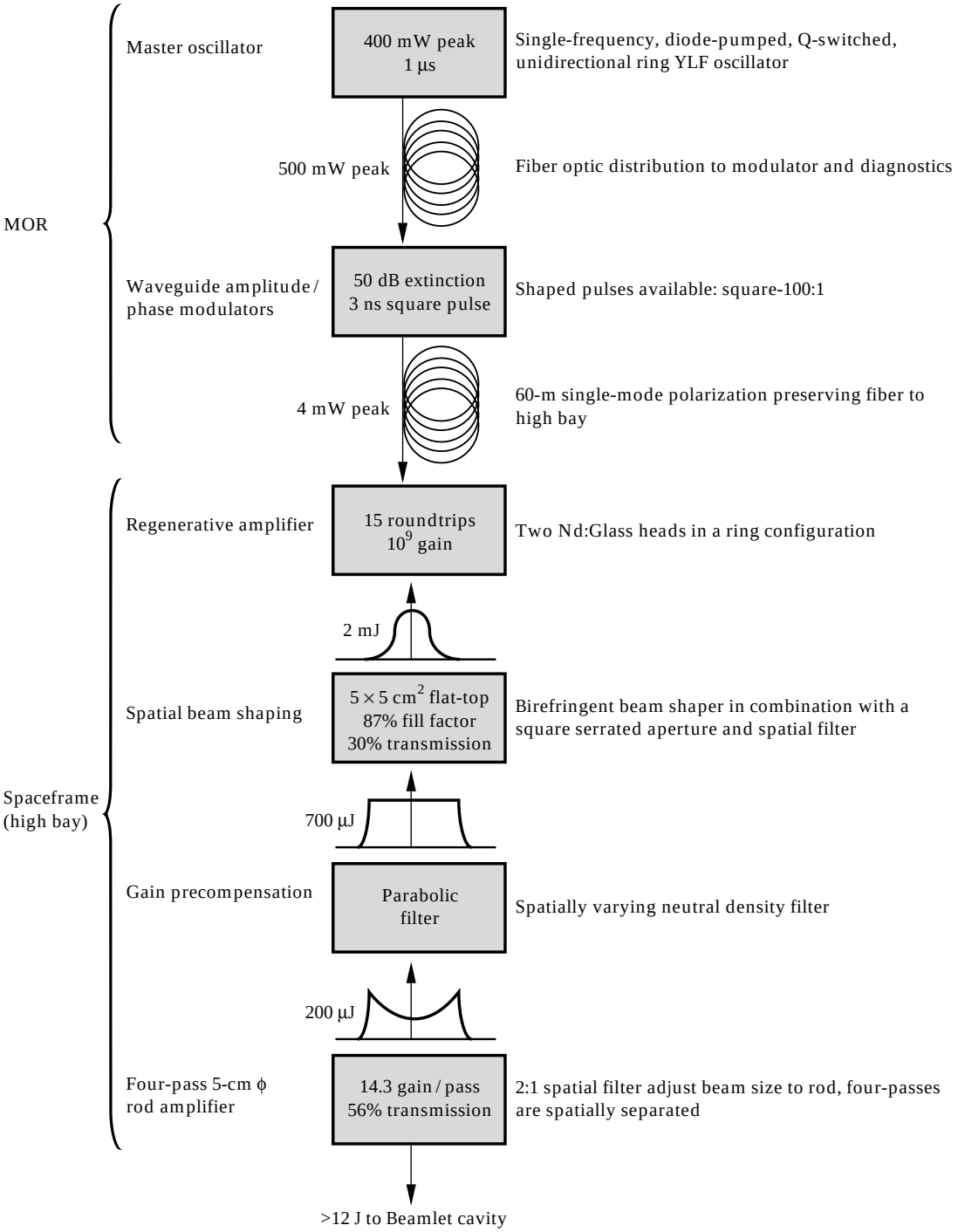

FIGURE 1. Schematic overview of Beamlet's front-end subsystems and how they interface. MOR means that this equipment is housed in the master oscillator room whereas all other front-end components are mounted on a spaceframe in the main laser bay. (70-50-0194-0033pb01)

back reflections from the main laser amplifier cavity. Then, the beam is incident on a 39-actuator deformable mirror (DFM) and relayed to the injection optics of the Beamlet cavity spatial filter.

Master Oscillator, Temporal Shaping, and Phase Modulation System Upgrades

Several upgrades and improvements have been implemented to the Beamlet master oscillator and modulator system since its initial description by Wilcox et al.[2] The original Nd:YLF microchip oscillator-amplifier system has been replaced by a very stable, compact, and powerful single-mode unidirectional ring oscillator.[3] A diode-pumped Nd:YLF crystal is used as a gain medium, while an acousto-optic Q-switch creates high-peak-power pulses and also serves as a direction-selective element for the three-mirror ring cavity [Fig. 2(a)]. The ring oscillator's higher peak power allows for optimization of the diagnostics and fail-safe systems. Figure 2(b) illustrates the complete oscillator, including the diagnostics and fiber couplers. Specifically, pulse shape and Fizeau bandwidth spectra can be monitored on a continuous basis. Additional fail-safe switches monitor the occurrence of beat modes and the magnitude of the bandwidth modulation created in the waveguide modulators.

The original $LiNbO_3$ amplitude modulator circuit continues to provide Beamlet with pulse widths ranging from 200 ps to 10 ns, and shapes as simple as Gaussian or as complex as the ignition pulse shapes required for NIF. (See "System Description and Initial Performance Results for Beamlet," p. 1.) The performance of the amplitude modulators has been significantly improved by a modification of the modulator bias control system. In the original system,[2] a DC bias voltage was used to optimize extinction of the amplitude modulators, but charge migration effects in the $LiNbO_3$ substrate resulted in a continuous drift of the desired bias point. The present system of short-pulse bias voltages results

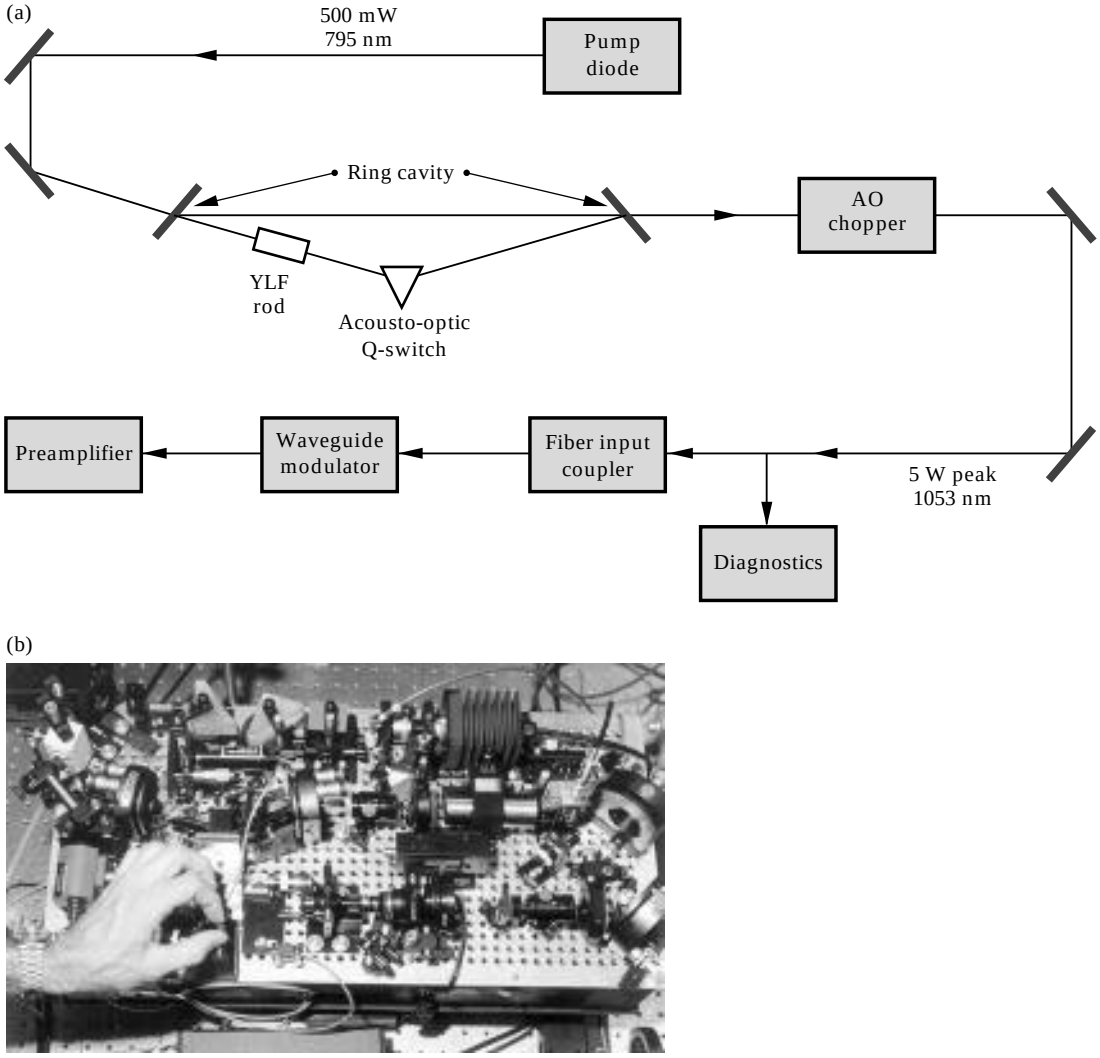

FIGURE 2. (a) Layout and (b) photograph of the new Beamlet unidirectional, single-frequency ring oscillator. The physical dimensions of the complete unit, including the pump-diode laser and diagnostics, are 30 cm × 60 cm; the size is six times smaller than the original oscillator, with a ten-fold increase in peak output power. (70-50-0494-1946pb01)

in optimum performance for extended periods of time without adjustments. The $LiNbO_3$ phase modulators easily provide Beamlet bandwidth requirements of 30 GHz at 1ω by using a single radio-frequency (RF) generator (with 3–6 GHz variable frequency output) and a power amplifier. Complex high-density sideband spectra have been demonstrated by driving the phase modulator with the sum of two different RF signals.

Stability requirements for the pulse-generation system are very demanding and several major stability problems have been recently solved. Using an all-fiber-optic polarization compensating device,[4] we reduced long-term fluctuations in the power delivered from the modulators to the regenerative amplifier in the preamplifier section by optimizing the polarization coupling in the long transport fiber. Another major source for shot-to-shot fluctuations is the gain instability of the flash-lamp-pumped amplifier heads in the ring regenerative amplifier. The instability of the output energy E_{out} is given by

$$\frac{\delta E_{out}}{E_{out}} \approx \frac{\delta E_{pump}}{E_{pump}} (\ln G) \quad , \tag{1}$$

where G is the total small signal gain (~10^9) and E_{pump} is the energy delivered by the flash lamps. It is clear from Eq. (1) that an unreasonably high pump stability of ±0.2% is required to maintain the output energy stable to within the required ±5%. To solve this stability problem, we implemented a new and elegant feed-forward stabilization scheme.[5] This scheme uses the existing pulse-slicer Pockels cell as a variable transmission element, controlled by a photoconductive Si switch. Light leaking through one of the regenerative amplifier cavity mirrors is used to control the conductance of the switch (Fig. 3). This scheme increased the shot-to-shot stability of the pulse-generation system to well within the operational requirements for Beamlet.

Spatial Intensity Profile Shaping

Beamlet's front-end spatial intensity shaping optics create the 2-dimensional (2-D) beam profile required for injection in the main cavity amplifier. First, the basic scheme uses a set of birefringent filters to flatten the Gaussian regenerative amplifier beam profile (Fig. 4). Next, the beam passes through a square serrated aperture with rounded corners; this generates a well-defined square edge profile of the beam.[6] The serrated edges of the aperture need to smoothly reduce the beam intensity from its peak to near zero to avoid diffraction ripples on the transmitted beam. However, the width of the serrated edge needs to be sufficiently narrow to guarantee a high fill factor of the beam. Fill factor is defined as the ratio of the power in the actual beam to the power of an equivalent beam that completely fills (100%) the same area. (Note that to completely fill the area the intensity profile at the edge of the beam is discontinuous, i.e., infinitely steep.) Beamlet uses an inverted Gaussian serrated edge profile with a width equal to 10% of the beam size. A new type of serrated aperture, produced by a photolithographic process, resulted in a significant improvement of quality and uniformity of the beam edge profile as shown in Fig. 5. Using this procedure, the shape of the serrations can be controlled to within a precision of 2 μm. The resulting fill factor of the Beamlet output beam exceeds 84% when integrated between the 1% intensity points at the edge of the beam profile.

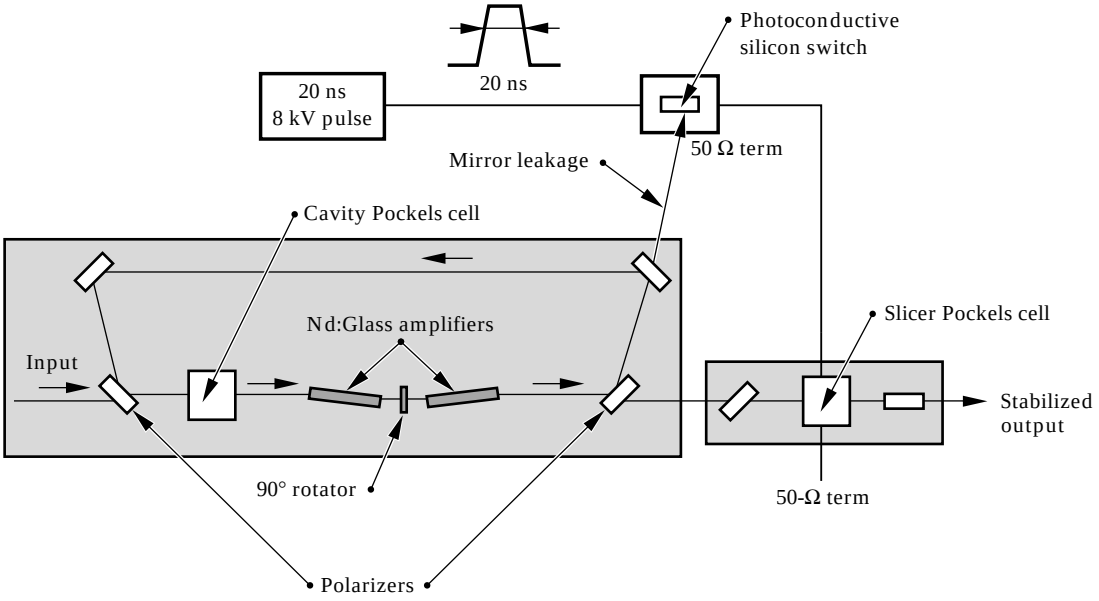

FIGURE 3. The existing pulse slicer behind the regenerative amplifier was modified to a feed-forward energy stabilization system. Light leaking through one of the regenerative amplifier cavity mirrors illuminates a Si photoconductive switch in the Pockels cell driver line, providing negative feed-forward control of the pulse slicer Pockels cell's energy transmission. (70-50-0295-0400pb01)

A major improvement in Beamlet performance is achieved by shaping the spatial intensity profile of the pulse generated by the front end to compensate for spatial gain variations in the main Beamlet multisegment amplifiers. Spatial variations in the gain of the amplifiers result from amplified spontaneous emission within the laser slabs. Briefly, amplified spontaneous emission trapped within the laser slab by total internal reflection depletes the stored energy in the glass, particularly near the edges of the slabs. This depletion in stored energy produces a corresponding roll-off in the gain, largely in the horizontal direction. (See "Design and Performance of the Beamlet Amplifiers," p. 18.) The resulting small signal gain for the combined 44 slabs that the beam traverses during a Beamlet shot resembles a parabola with center-to-edge gain ratio in the horizontal direction exceeding 3.5. Therefore, if a beam with a flat-top intensity profile is injected into the main laser cavity, then the output beam profile will roll off at the edges in the same way as the overall gain profile. This greatly reduces the fill factor. For a system designed to run at beam fluences near the damage threshold of its optical components, a reduction of fill factor reduces the maximum output energy available. Gain saturation at very high output fluences (>>10 J/cm^2) tends to reduce this effect. However, the system fluence limit can be located at nonsaturated points in the amplifier, such as the Beamlet cavity polarizer (its limiting fluence is 11 J/cm^2). Precompensating the lower gain near the edges by increasing the intensity of the injected profile counteracts this effect, as shown in Table 2, where we compare the total modeled output energy at fixed peak fluence with, and without, precompensation for the gain nonuniformity.

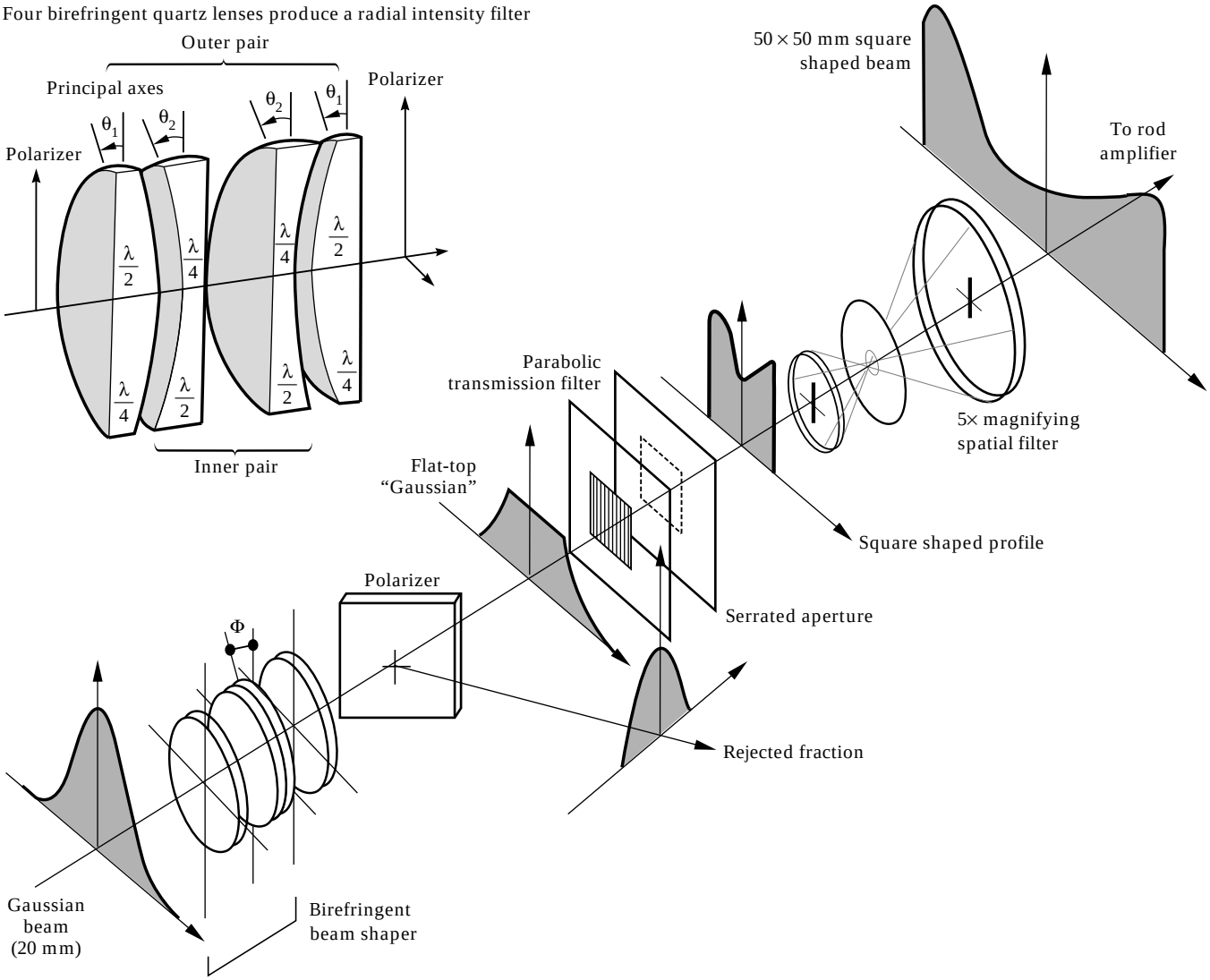

FIGURE 4. The spatial profile of the Beamlet injection pulse is generated in a three-step process in the beam-shaping section: (1) The beam is converted from Gaussian to a flat-topped round beam; (2) the beam is converted to a square footprint using a serrated aperture; and (3) a parabolic profile is created using a special transmission filter. The beam shaping section is located between the regenerative amplifier and the four-pass rod amplifier. (02-07-0892-2883pb01)

(a) Details at the beam's edge

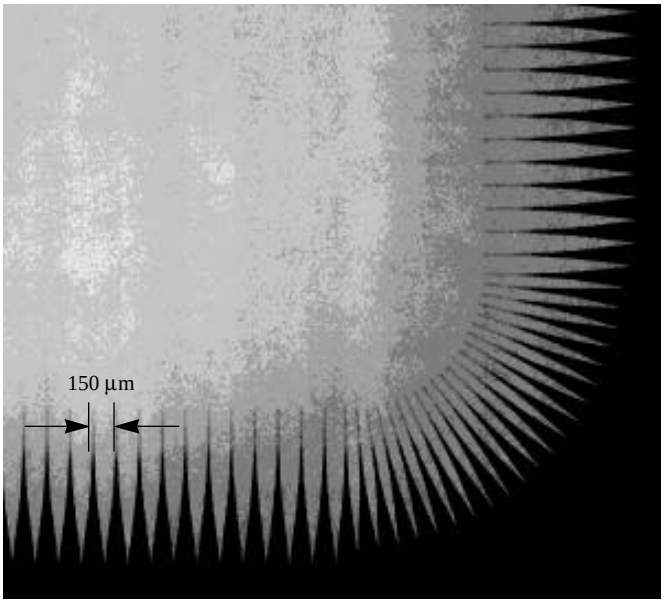

(b) Full-aperture display

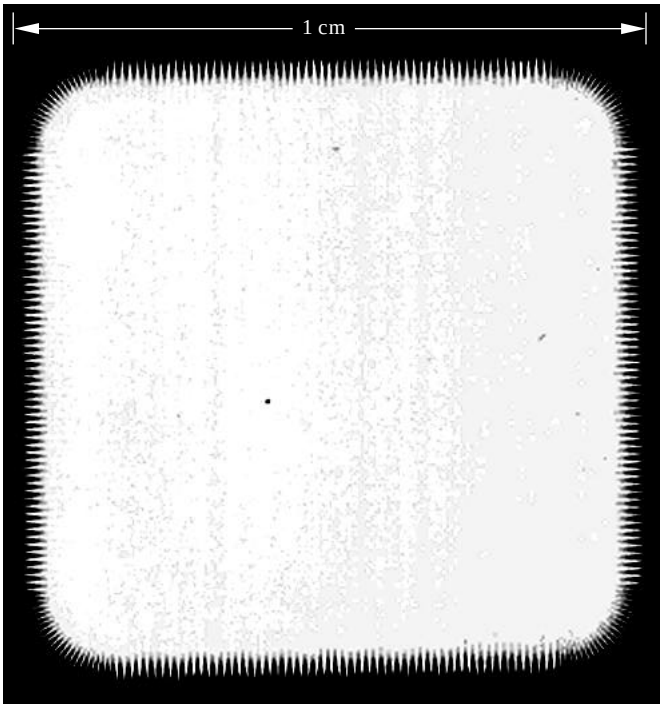

FIGURE 5. A smooth yet rapid roll-off in the intensity profile at the edge of the beam is created using precisely shaped serrations in a photolithographically created pattern. The low-pass spatially filtered image of this aperture is relayed through the main amplifier onto the frequency-conversion crystals. (70-10-1193-3899pb01)

Various methods exist to shape a beam's intensity profile, ranging from simple spatially varying neutral density filters to afocal refractive optical systems and complex high-resolution programmable spatial light modulators. We use the first method on Beamlet. Figure 6(a) compares an actual profile with the specified transmission profile for a shaped neutral density filter.

(a) Transmission scan

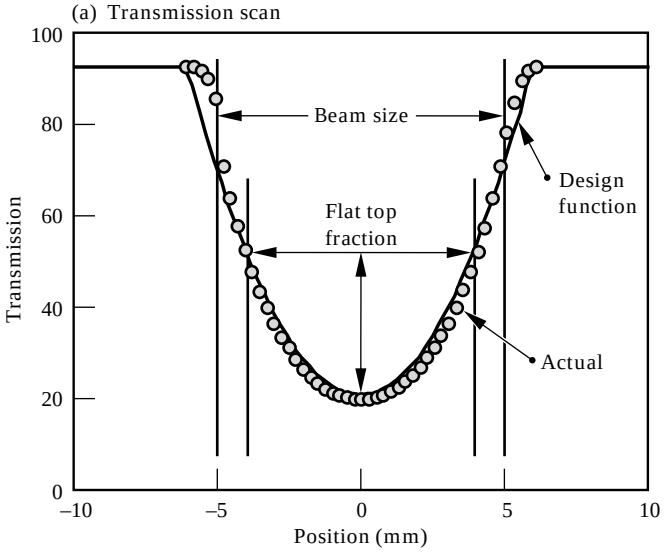

(b) Resulting beam profile

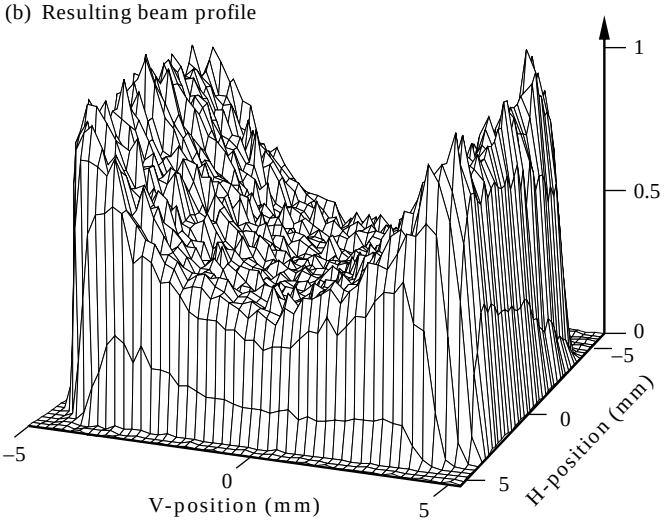

FIGURE 6. (a) Experimental transmission scan of a parabolic 1-D transmission filter compared with the specified transmission curve. The relevant beam size dimensions are overlaid. (b) A 2-D plot of the resulting beam profile measured at the 1ω output diagnostics station for an unpumped amplifier cavity. (70-50-0295-0401pb01)

TABLE 2. Shaping the intensity profile of the injected beam improves the output energy.[a]

Output fluence (Beamlet 11-5)	Output energy flat profile	Output energy shaped profile	Improvement with shaped profile
8 J/cm^2	6.8 kJ	8.2 kJ	21%
10 J/cm^2	8.7 kJ	10.2 kJ	17%
12 J/cm^2	10.8 kJ	12.3 kJ	13.6%

[a]Beamlet baseline, 11-5 configuration, 0.20 explosion fraction, f_x, 34 cm × 34 cm^2 beam.

The filters are created using variable-speed computer-controlled e-beam deposition of Cr on a BK-7 glass substrate. The filter's parabolic transmission profile is slightly wider than the actual beam size, allowing the profile of the transmitted beam to be adjusted to match the slightly skewed Beamlet amplifier gain profile. Figure 6(b) shows the near-field intensity profile of the beam transmitted through this filter and then propagated through the entire *unpumped* amplifier chain and measured at the 1ω output diagnostic station. Figure 7 shows the output near-field profile using the same parabolic transmission filter *pumping* the amplifiers; note the desired flat-top output profile that is achieved. These results are discussed further in the "System Description and Initial Performance Results for Beamlet," p. 1.

Compensation for gain nonuniformity in the amplifiers has a second advantage—it decreases any spatially dependent pulse-shape distortion produced by the main amplifiers. The temporal pulse shape distortion, caused by gain saturation at high fluences during the last pass through the cavity and the booster amplifier, is homogenous because of the fluence uniformity. If the beam is not corrected for spatial gain variations, then it will have lower fluences near the beam edges, and hence will undergo different temporal pulse distortions near the edges than near the center of the beam. The result is that the output temporal profile will be different at the edges of the beam than at the center. Therefore, by correcting for spatial gain variations in the main amplifiers we also produce a uniform-pulse temporal profile across the full aperture.

Wavefront Shaping Using the Adaptive Optics System

The wavefront of a laser beam governs how well the beam propagates. Since rays of light always travel perpendicular to the local wavefront, the wavefront determines whether the laser beam is diverging, converging, collimated, or is generally deforming in shape and size and breaking up. In Beamlet, the wavefront determines the size of the beam's focus and how the energy is distributed at the focus. In addition, the wavefront determines how much of the light is within the acceptance angle for conversion to shorter wavelengths, which impacts the conversion efficiency of the light from the fundamental wavelength at 1054 nm to the third-harmonic wavelength at 351 nm. The Beamlet Type I / Type II frequency converter requires 95% of the 1ω energy be within a divergence angle of ±50 µrad. The beam divergence requirement needed to meet the NIF focusability requirement is much more stringent: 95% of the 3ω energy needs to be within a ±35-µrad divergence angle. Beam divergence is caused by the static aberration of the individual optics surfaces, pump-induced spatially varying beam steering in the amplifiers during a shot, thermal aberrations in hot amplifier slabs, and turbulence in the heated amplifier cavity. Table 3 provides an overview of the various aberrations, the associated time scale on which they occur, and the spatial scale length. The correctability constraints are imposed by the choice of actuator density and control system speed. Both factors can be increased significantly beyond the performance of the system used on Beamlet.

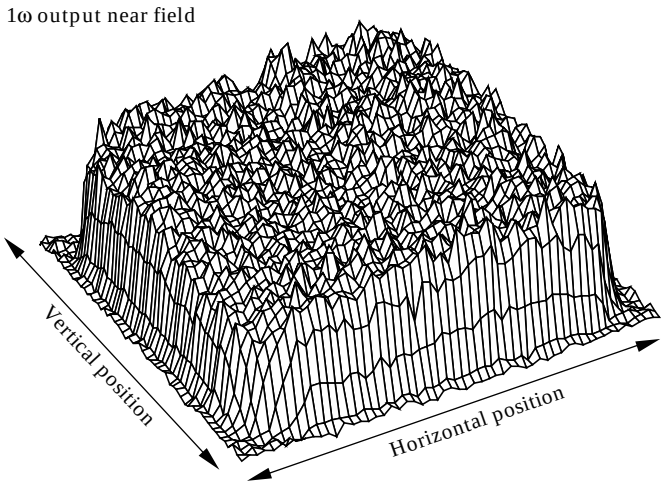

FIGURE 7. Example of the approximately flat-topped near-field intensity profile achieved at the output of the Beamlet amplifier chain using the parabolic gain compensation filter described in the text and shown in Fig. 6(b). (70-50-0295-0594pb01)

TABLE 3. Factors affecting Beamlet's wavefront quality, and the ability to correct for these factors using the 39-element DFM.

Factor	Magnitude of aberration (waves)	Temporal dependence	Aberration spatial scale[a]	Correctability[b]
Optics figure errors	2.5	Static	d / 4	Excellent
Pump induced	2.5–3	50 µs	d / 4	Good
Thermal effects in slabs	2.5–6	4 hr	d / 3	Excellent
Turbulence in amps[c]	0.5–1	Seconds	d / 10	Marginal
Small scale errors	0.01–0.2	Static	<d / 10	Not possible[d]

[a]d represents the beam size.
[b]Using the present Beamlet DFM hardware.
[c]Turbulence due to thermally driven convection currents.
[d]Limited by the choice of actuator density.

The Beamlet adaptive optics system is designed to correct the wavefront of the laser beam to be nearly "flat," i.e., to as near a plane wave as possible. As mentioned earlier, this maximizes the conversion efficiency of the fundamental IR beam to the UV and minimizes the size of the focus spot, thus maximizing the power density at the target. The adaptive optics system, shown schematically in Fig. 8, consists of a DFM, a wavefront sensor, and a controller. The design is based on an adaptive optics system developed by Salmon et al.[7] for laser isotope separation. The DFM is located in front of the injection spatial filter for the main multipass amplifier. The light is sampled by the wavefront sensor after the DFM, and the controller analyzes the wavefront from the wavefront sensor and drives the DFM until the sensor reads the desired wavefront, which is flat for Beamlet. The DFM is comprised of a single thin-glass substrate with 39 magnetostrictive actuators bonded to its back side. The mirror substrate is 70×70 mm^2 wide and 4 mm thick. Its front surface is coated with a low-stress HfO_2/SiO_2 high-damage-threshold and high-reflectivity multilayer coating (Fig. 9). The arrangement of actuators divides the mirror surface into grids of subapertures, each subaperture being the smallest area

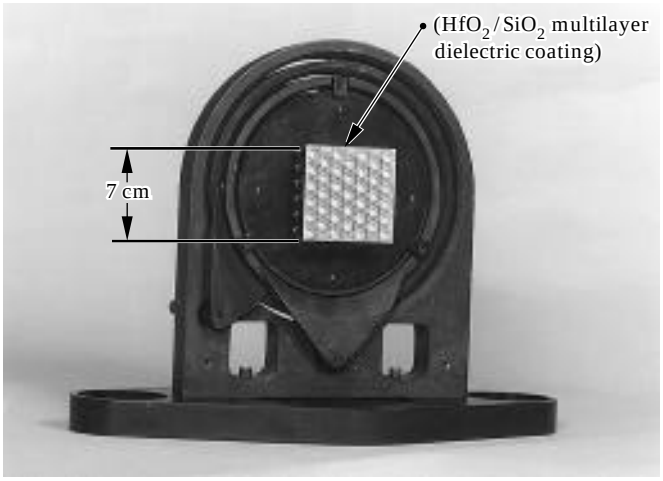

FIGURE 9. The Beamlet DFM has 39 actuators mounted to the back of a $70 \times 70 \times 4$ mm^3 coated substrate. The range of motion of individual actuators is approximately 10 μm. (70-50-0494-2093pb01)

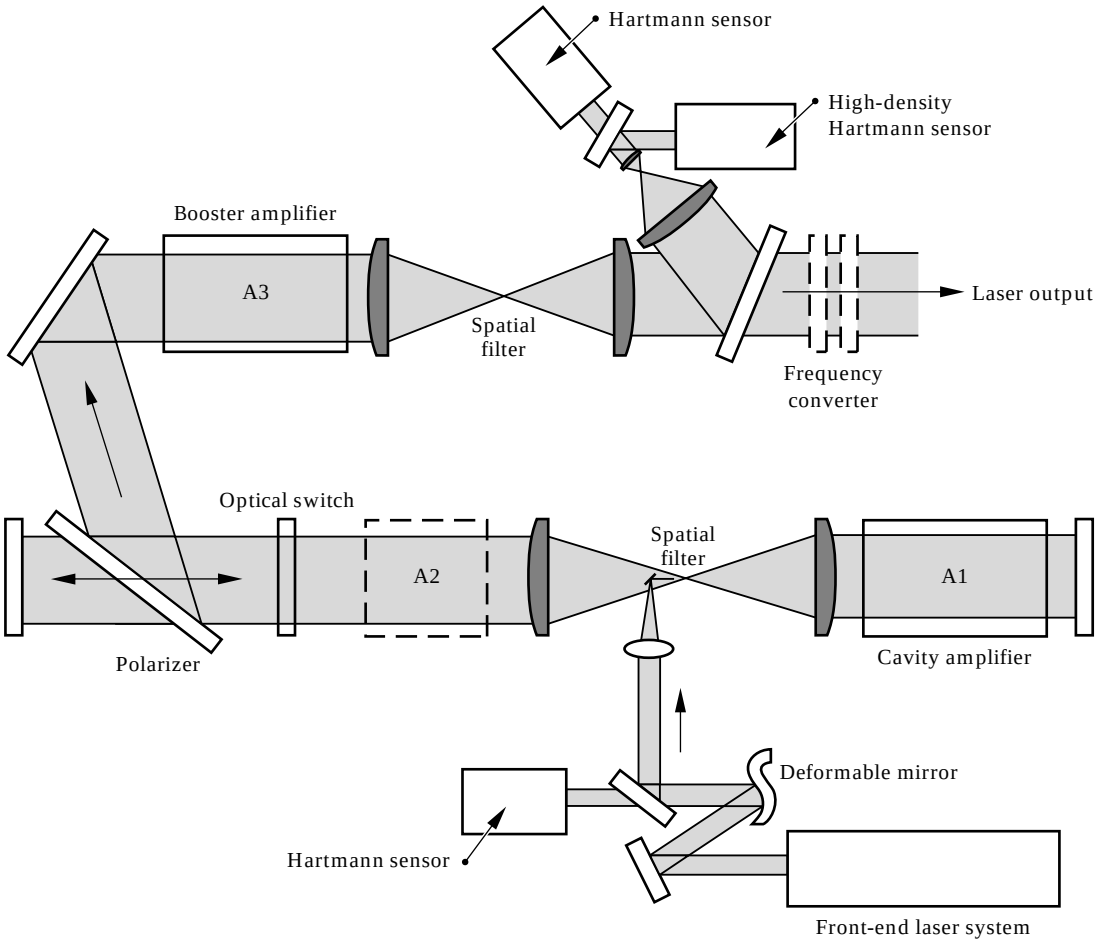

FIGURE 8. Beamlet adaptive optics system layout: a DFM located in the injection beam path is operated by a control system. This system operates in closed loop to a Hartmann wavefront sensor in the injection path (flat injection wavefront), or in the 1ω-output diagnostics of the Beamlet amplifier (flat output wavefront). An additional higher spatial resolution Hartmann sensor is located in the output diagnostics. (70-50-0295-0402pb01)

that is enclosed by a group of adjacent actuators. Each actuator expands when a voltage is applied and produces a local bulge in the front surface opposite the actuator, while the neighboring actuators hold the mirror surface in place. This movement causes the mirror surface to tilt across the subapertures, adjacent to the moving actuator. The wavefront change, induced by the movement of a single actuator, is called the influence function. The influence function is usually Gaussian shaped, with its $1/e$ point located at the neighboring actuator.

The wavefront sensor is a Hartmann sensor, which has a series of lenses that collectively "view" the entire surface of the DFM. Figure 10 shows the relationship between the DFM actuator positions and the Hartmann sensor lenslets. Each lenslet spans a subaperture of the DFM and is configured as a local pointing sensor for that subaperture, i.e., the detector for each lenslet is in the focal plane of that lenslet. As the tilt in the wavefront of light entering the Hartmann lenslet changes, the focus spot on the detector moves laterally from its nominal position on the detector. Moving any actuator will cause the Hartmann spots to move from their nominal positions. Knowing how the spots move when each actuator is moved, the controller can drive the DFM until the displacement of the Hartmann spots is minimized, thus minimizing the wavefront error sensed by the Hartmann sensor.

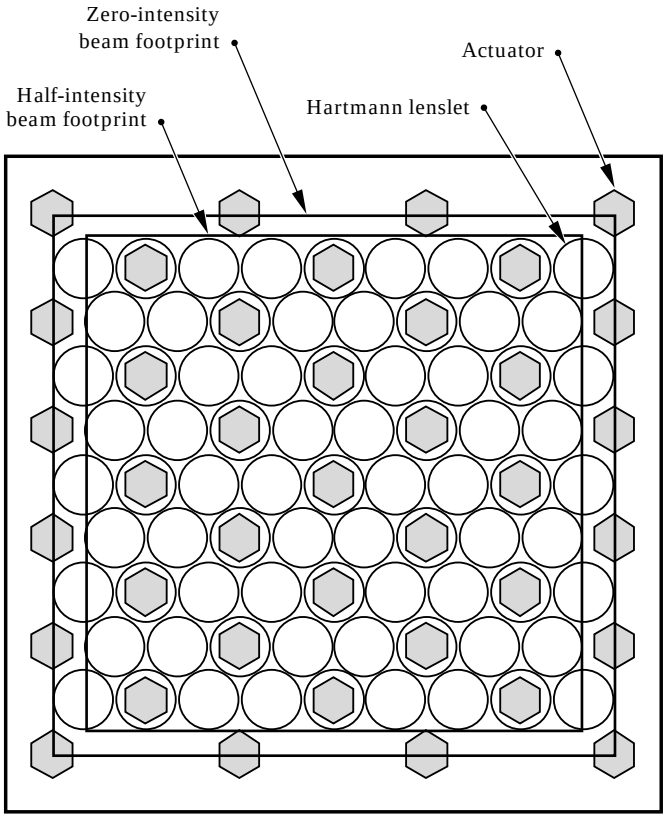

FIGURE 10. Layout of the 39 actuators and the 77 Hartmann sensor lenslets mapped onto the DFM surface. (70-50-0295-0403pb01)

The system uses two Hartmann sensors—one to sample the light immediately after the DFM (input Hartmann sensor) and the other on the 1ω diagnostics table (output Hartmann sensor). Afocal telescopes relay the image of the DFM to each Hartmann sensor, and each Hartmann sensor is calibrated by a wavefront reference source. The wavefront calibration effectively removes any aberration introduced by either the afocal relay telescope or the beam sampler. The wavefront controller is designed to control the wavefront using either of the two Hartmann sensors. The bandwidth for the closed-loop system is about 1/2 Hz for continuous wave (cw) light and about 1/50 Hz for regenerative amplifier pulses. A third Hartmann sensor is installed in the output diagnostic station. It is used for wavefront characterization measurements and provides a higher resolution than the control system sensors. It has a larger density of lenslets over the beam aperture (17×29).

As presently configured, the adaptive optics system can correct the wavefront using either cw light from the alignment laser or a 0.2-Hz pulsed beam from the regenerative amplifier. Precorrection of the injected wavefront to compensate for pump-induced aberration in the amplifier proceeds as follows: (1) The wavefront is flattened before a shot by running the control system closed loop to the output Hartmann sensor using the alignment laser. (2) The Hartmann sensor images are grabbed during the laser shot, and the resulting aberrated wavefront is reconstructed offline. (3) Before the next shot, this wavefront is entered in the control system that subsequently sets the mirror in closed loop such that the output wavefront is the conjugate of the shot wavefront error. The wavefront aberration of the shot should be corrected for pump-induced aberrations. Figure 11 shows recent wavefront data to illustrate this process. Two situations are depicted: the wavefront of a shot with static precorrection only, and a shot where full precorrection is applied. The wavefront shape is typical of the pump-induced wavefront aberration by the Beamlet amplifier slabs added to a focus error in the front-end rod amplifier. Its shape and magnitude agree closely with model predictions and offline beam-steering characterization data. (See "Design and Performance of the Beamlet Amplifiers," p. 18.) The second wavefront is the result of a shot where full precorrection for the errors shown in Fig. 11(a) is applied. The rms value of the resulting aberration is <0.2 waves, leading to a Strehl ratio (ratio of actual peak intensity of the focal spot to the diffraction limited peak intensity) of 0.3. The correction capabilities are presently limited by turbulence-induced wavefront variations between the time of prefiguring the DFM and the actual shot. This effect is small in a cold cavity, but becomes substantial after firing subsequent shots at the nominal 2-hr Beamlet shot rate.

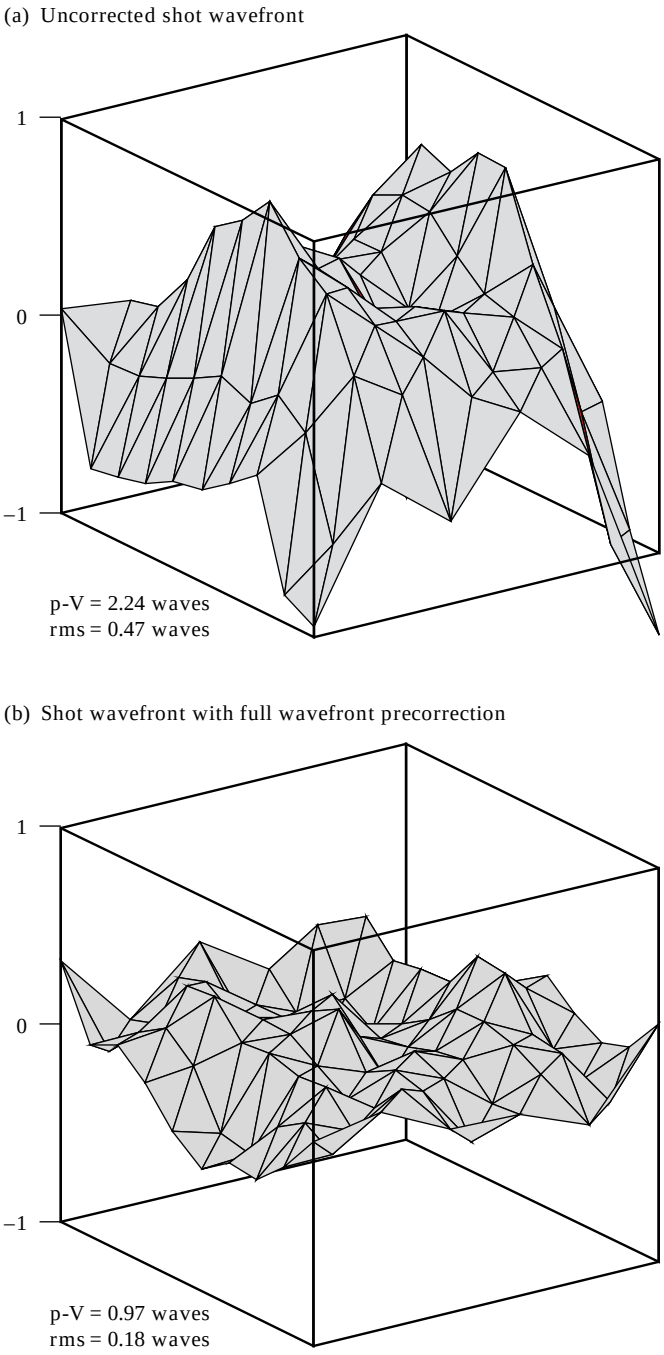

FIGURE 11. Experimental output high-resolution Hartmann sensor wavefronts obtained during 4.5-kJ 3-ns Beamlet shots (34 cm × 34 cm^2 beam). (a) The typical pump-induced wavefront aberration in the Beamlet amplifiers. (b) The output wavefront of a shot with full precorrection of the injected wavefront for static and dynamic aberrations in the Beamlet amplifier. The resulting 0.18 waves rms aberration correspond to a calculated Strehl ratio of 0.3. (70-50-0295-0404pb01)

Summary

We added the capability to control the spatial intensity profile and wavefront of the pulse produced by the Beamlet pulse-generation system (i.e., front end). We also demonstrated how these capabilities can be used to control and increase the beam quality and performance of Beamlet's large-aperture multipass Nd:Glass amplifier—a technology critical to the design of the proposed NIF laser system.

In addition, we have also modified and improved the front-end oscillator and modulator systems to increase the stability and reliability of their performance.

Notes and References

1. B. M. Van Wonterghem, D. R. Speck, M. J. Norman, et al., *ICF Quarterly Report* 3(1), 1–9, Lawrence Livermore National Laboratory, Livermore, CA, UCRL-LR-105821-93-1 (1993).
2. R. W. Wilcox and D. F. Browning, *ICF Quarterly Report* 2(3), 115–122, Lawrence Livermore National Laboratory, Livermore, CA, UCRL-LR-105821-92-3 (1992).
3. L. J. Bromley and D. C. Hanna, *Opt. Lett.* 16(6), 378 (1991).
4. H. C. Lefevre, *Electronics Letters* 16(20), 778 (1980).
5. R. W. Wilcox, US Patent No. 5,157,676.
6. J. M. Auerbach and V. P. Karpenko, *Appl. Opt*., 3179–3183 (1993).
7. J. T. Salmon, E. S. Bliss, T. W. Long, et al., *Active and Adaptive Optical Systems* (SPIE—International Society for Optical Engineering, Bellingham, WA, 1991; *Proc. SPIE* 1452) pp. 459–467.